Proceedings of IMECE12
2012 ASME International Mechanical Engineering Congress and Exposition
November 9-15, 2012, Houston, Texas, USA

IMECE2012-88417

PERFORMANCE IMPROVEMENT OF A WIND TURBINE BLADE DESIGNED FOR LOW WIND SPEEDS WITH A PASSIVE TRAILING EDGE FLAP

Mohammed Rafiuddin Ahmed
Division of Mechanical Engineering
The University of the South Pacific
Suva, Fiji

Epeli Nabolaniwaqa
Division of Mechanical Engineering
The University of the South Pacific
Suva, Fiji

ABSTRACT

The flow characteristics and the lift and drag behavior of a newly designed thick trailing-edged airfoil that was provided with fixed trailing edge flaps (Gurney flaps) of 1% to 5% height right at the back of the airfoil were studied at different low Reynolds numbers (Re) and angles of attack for possible applications in wind turbines suitable for the wind speeds of 4-6 m/s that are common in the Pacific Island Countries. A thick trailing-edged blade section, AF300, that was designed and tested in a recent work for small horizontal axis wind turbines to improve the turbine's startup and performance at low wind speeds was chosen for this study. Experiments were performed on the AF300 airfoil in a wind tunnel at different Re, flap heights and angles of attack. Pressure distributions were obtained across the surface of the airfoil and the lift and drag forces were measured for different cases. It was found that the flap considerably improves the suction on the upper surface of the airfoil resulting in a high lift coefficient. For some of the angles, in the case of 3 mm and 4 mm flaps, the peak C_p values on the suction surface were significantly higher compared to those without the flap. However, at angles of attack of 12^o and above, this unusually high C_p on the upper surface close to the leading edge caused flow separation for some cases as the flow could not withstand the strong adverse pressure gradient. The CFX results matched most of the experimental results without flaps, except that the suction peak was lower numerically. The difference was higher for the case with flaps. It is clear from the results that trailing-edge flaps can be used to improve the performance of small wind turbines designed for low wind speeds.

INTRODUCTION

The superior aerodynamic performance of airfoils provided with Gurney flaps (GFs) is known for some time now. A Gurney flap is a small flat plate fitted on the pressure side of an airfoil at the trailing edge and perpendicular to the chord line. The GF was first used by Dan Gurney on his race car to improve the aerodynamic downforce; he observed that the flap increased the downforce and slightly reduced the drag force [1]. The GFs have attracted a lot of attention for some time due to their effectiveness from a simple configuration [1,2]. Studies on airfoils fitted with Gurney flaps have also been performed for wind turbine applications [3-5]. The GF influences the aerodynamics of the airfoil significantly by shifting the location of flow separation, altering the trailing-edge flow conditions and effectively changing the camber [6]. They induce vortices that turn the flow and as a result, enhance the suction on the suction side and increase the pressure on the pressure side [7]. The maximum lift coefficient was observed to increase by up to 30% [1,8].

Several researchers have investigated the optimum size of GF in an attempt to maximize the lift to drag ratio of airfoils. The general consensus seems to be that the best size of the GF depends on the thickness of the boundary layer near the trailing edge; the boundary layer thickness should be greater than the GF height [9]. Maughmer and Bramesfeld [8] performed a thorough experimental investigation of the effect of fitting GF to a 12% thick airfoil. They recorded a reduced suction peak at an angle of attack (α) of about 5^o (corresponding to a C_l of 0.7) while there was an increase in the lower surface pressures near the trailing edge. On the other hand, at the angle of attack of $C_{l,max}$, the flow separation from the upper surface got delayed due to the 2% flap and the lower surface pressure increased after half the chord length. It has generally been reported that the optimum height of the GF is 2% of chord [7].

Research efforts directed at maximizing the power output of wind turbines have increased significantly during the recent years. The commonly used NACA airfoils are found inappropriate for wind turbines that are required to operate in regions of low wind. The NACA airfoils are suitable for

applications where the Reynolds numbers (Re) are high and the angles of attack are relatively small [10,11]. Attempts are being made to develop good airfoil geometries that are appropriate at low Re for energy extraction from the wind at low wind speeds. The rotor blade is one of the most important parts of the wind turbine which is the primary energy conversion device. For the wind turbine blade design, the selection of airfoils for different sections and the distribution of chords and twists are pivotal [12]. A number of sites in many countries have locations where the wind speeds are not very high. As the aerodynamic efficiency increases with tip speed, advances in the development of small wind turbines will provide solutions to the energy requirements of many countries. Researchers have been trying to make performance data sets of representative airfoils available, which will help in validating prediction codes used for design purposes [13,14].

The present investigation is a part of the work undertaken to design our own airfoils for specific applications. The airfoil, which has a thick trailing edge, was designed and tested at different low Re [15]. In the present work, fixed GFs of heights 1% to 5% of the chord were provided just behind the thick training edge. The advantage of using thick trailing-edged airfoil in such studies is that the new concept of deployable GFs (MiTEs) can easily be implemented by either retracting the flap completely or extending it on the upper surface if mitigation in the lift is required [6]. With the present airfoil, all the three flap positions of up, neutral and down can be realized depending on the required output from the turbine.

The freestream turbulence levels of the atmospheric wind at heights at which wind turbines are normally installed are generally higher than the levels achieved carefully in standard wind tunnels. The airfoil characteristics are known to change with freestream turbulence level [16-20]. Hoffmann [16] studied the effect of variation of the freestream turbulence intensity from 0.25% to 9% for NACA0015 airfoil at Re = 250,000 and reported an increase in $C_{l,max}$ due to delayed flow separation at higher angles of attack. Swalwell et al. [17] varied the freestream level from 0.6% to 7% and studied the pressure distribution and lift and drag characteristics for NACA0021 airfoil. Devinant et al. [18] varied the turbulence level from 0.5% to 16% and studied its effect on NACA 65_4-421; they found that the flow was separating at higher angles of attack when the turbulence level was increased. Maeda et al. [19] studied the effects of turbulence intensity on the static and dynamic characteristics of DU93-W-210 airfoil at Re = 350,000 at two turbulence levels of 0.15% and 11%. They also found that the flow separation gets delayed at higher turbulence levels and the stall angle gets increased. Sicot et al. [20] varied the turbulence level from 4.4% to 12% and studied the effect on the lift, drag and power output characteristics of a NACA65_4-421 profiled blade. Thus, it is clear that most of the works on such studies are done on NACA airfoils with sharp trailing edge. Based on the above-mentioned works and their findings and the fact that the turbulence levels at lower altitudes and in the wake of other wind turbines (for wind farm applications) varies in this range [21], it was decided to investigate the effect of turbulence levels by also studying some of the airfoil characteristics at the turbulence intensity of 10%.

With a sudden change in the turbulence intensity of the wind, the flow structure over the blade changes significantly, shifting the location of transition as well as that of separation. Therefore, it is advisable to choose a profile that has the upper surface transition point close to the leading edge at the design angle of attack [22].

This paper presents the results from a detailed study of GFs, in which the performance characteristics of a low Re, thick trailing-edged airfoil are studied at different freestream velocities, angles of attack and two turbulence levels, both experimentally and numerically and attention is focused on α and Re values which are appropriate as design points. The experimental work was carried out in a low speed wind tunnel and the numerical simulation was performed using the package ANSYS-CFX. The GFs are known passive devices for improving the performance of airfoils and blades. However, the mechanisms responsible for the enhancement in the performance are not yet fully understood [2]. Hence, the present work is intended to gain further insight into the aerodynamic characteristics of a thick trailing-edged airfoil with GFs of different heights.

NOMENCLATURE

A	airfoil planform area = c × span
c	chord length
C_l	coefficient of lift = $L/q_\infty A$
C_d	coefficient of drag = $D/q_\infty A$
C_p	coefficient of pressure = $(p - p_\infty)/q_\infty$
D	drag force
L	lift force
p	static pressure at a point
p_∞	freestream static pressure
q_∞	freestream dynamic pressure
Re	Reynolds number = $\rho U_\infty c/\mu$
Tu	turbulence intensity = $\sqrt{0.5(\overline{u'^2} + \overline{v'^2})}/U_\infty$
u’	fluctuation in streamwise velocity
v’	fluctuation in transverse velocity
U_∞	freestream mean velocity
x	distance along chord from the leading edge
x_{tr}	distance from the leading edge to the location of transition
α	angle of attack
μ	dynamic viscosity
ρ	air density

EXPERIMENTAL METHOD

Wind Tunnel and Airfoil

The experiments in this work were performed at three different Reynolds numbers in an open circuit, suction type,

low subsonic speed wind tunnel at the University of the South Pacific. The airflow in the tunnel was generated by a centrifugal flow fan having a rated discharge of 4.53 m^3/s at the pressure of 996.7 Pa and the speed of 2253 rpm. The fan is driven by a thyristor controlled 10 HP AC motor. A settling chamber, provided with honeycomb gauges and three high-porosity screens, was used for correcting the flow. A bell-mouthed inlet section ensured smooth entry of the air to the settling chamber. The airflow was discharged into the test section through the square outlet of the contraction. The area ratio of the contraction nozzle is 6.25:1. A smooth variation in velocity from 3 m/s to 50 m/s can be achieved in the test section having dimensions of 303 mm x 303 mm x 1000 mm. The test section is provided with perspex windows on both sides. A traversing mechanism is provided on top of the test section for moving the pitot-static tube and hot-wire anemometer probe along its length in the mid-span plane of the test model. The freestream turbulence intensity in the test section was found to be about 0.8% at the highest velocity and was of the order of 1% in the Re range of interest.

Measurements of surface pressures were carried out with a Furness Controls Micromanometer (model FCO510) having a range of ±19620 Pa. The Micromanometer was calibrated against a U-tube water manometer. The lift and drag forces were measured with a dynamometer.

The low Re AF300 airfoil, investigated in the present work, has a maximum thickness of 12% and a camber of 7% (maximum camber located at 47% of chord); the training edge thickness is 3%. Thick trailing-edged airfoils provide both structural and aerodynamic advantages over sharp trailing-edge airfoils. They reduce the adverse pressure gradient on the upper surface by allowing part of the pressure recovery to take place in the wake region and reduce the chances of early separation for both clean and soiled conditions and improve lift performance [23]. The airfoil was made out of wood in the laboratory. Pressure taps, perfectly flush with the surface, were provided on the upper and lower surfaces of the airfoil. Forty one pressure taps were used to measure the pressure distribution. The experiments were repeated a number of times on airfoils of chord lengths (c) 75 mm and 100 mm. Figure 1 shows a picture of the pressure taps on the airfoil while Fig. 2 shows the geometry of the airfoil with a flap.

Experimental procedure

The required mean velocity was set with the help of the thyristor system. Experiments were carried out at three Re of 100,000, 158,000 and 250,000 based on the chord length and the corrected freestream velocity. Most of the contribution to the lift force comes from the region slightly inboard from the tip where the Re is of the order of 150,000-200,000 for smaller turbines under consideration for a tip speed ratio of about 5 and normal rotational speeds. The attention of the study is focused on angles of attack up to 16°. In most cases, it is desirable that the design α-region is close to the maximum value of lift coefficient ($C_{l,max}$).

The freestream velocity was set for the required Re values at different values of α. The constant chord length blade was placed horizontally in the test section and it spanned the width of the test section. The axial location of the leading edge was only 10 cm from the exit of the contraction. In view of this, the very small flow component towards mid-span due to the boundary layer on the side walls of the test section does not affect our pressure measurements as the pressure taps were provided near the mid-span of the test model, thus providing a two-dimensional flow over the pressure taps (airfoil characteristics).

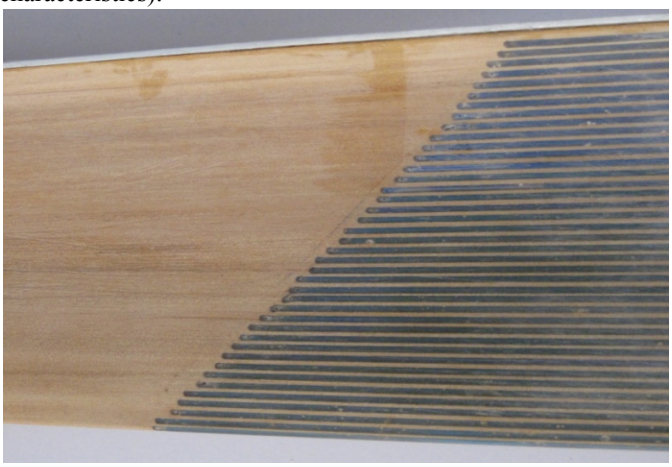

Fig. 1. A picture of the pressure taps on the AF300 airfoil

Another airfoil with a slightly shorter span was used for making lift and drag measurements. The angle of attack was varied from 0° to 16° and the pressure measurements were performed. The freestream turbulence level was varied by changing the turbulence screens before the contraction and the scale of turbulence was smaller compared to the chord length of the airfoil. The measured freestream velocity was corrected for solid and wake blockages [24]. The pressures were converted to the pressure coefficient (C_P). The accuracy of C_P measurements was estimated to be ±1.9%, while the repeatability was ±1.82%.

COMPUTATIONAL METHOD

The AF300 airfoil geometry was imported into the pre-processor. The domain was chosen such that a minimum distance of 15 times the chord length of the airfoil was maintained from the airfoil to the edges. The airfoil was located in the middle of the domain. The geometry was meshed using the software ICEM-CFD. The mesh is based on structured O-grid and C-grid topology and properly resolves the boundary layer, the size of cells adjacent to the walls is limited by $y+ < 1$. The resulting size of the mesh is 500000 nodes. Turbulent flow solution was used in ANSYS CFX and the turbulence modeling was done with κ-ω based SST model. The transition modeling was done with 'Gamma Theta Model'. The inlet velocity was varied to get the desired Re based on the airfoil chord length. The freestream turbulence level of the incoming air was set at 1% and 10% to study the effect of turbulence intensity, as discussed earlier. For convergence, residual type of RMS and the residual target value of 1×10^{-6} were set as the criteria. The

geometry of the airfoil with the 3% GF as well as the zoomed-in meshing around the airfoil can be seen from Fig. 2.

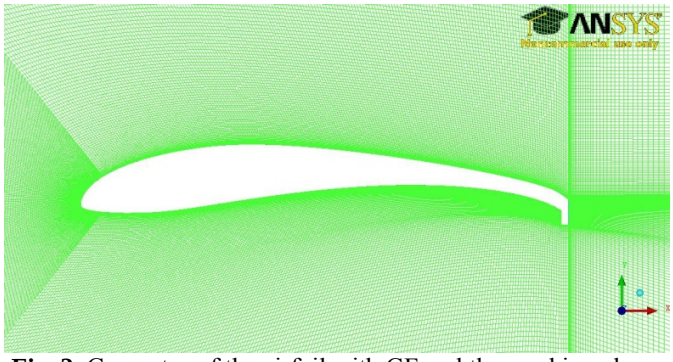

Fig. 2. Geometry of the airfoil with GF and the meshing close to the airfoil

RESULTS AND DISCUSSSION

The results are presented and discussed in this section. Figure 3 shows the experimental pressure distributions on the surface of the airfoil for $\alpha = 0^o$ and Re = 158,000 for the cases without flap and with GFs of heights 1% to 5% in increments of 1%. Most of the pressure distribution plots are shown for this Re as it was found that the trends for the pressure distributions do not change significantly at the other two Re. For the calculation of C_P, the measured static pressure at a point was non-dimensionalized with respect to the freestream static pressure and the corrected freestream velocity. The freestream turbulence intensity was 1% in this case. The results of the pressure distribution without GF from CFX computations are also included for comparison. It can be seen that the numerical results match the experimental results well except for the region close to the leading edge where the experimental Values of C_p were higher compared to the numerical values. It can be seen that the GF significantly improves the suction on the upper surface. The magnitude of maximum suction (minimum C_p) almost doubled with the GF, with the 4% GF showing the maximum suction, followed by 3%, 2% and 1%. Interestingly, the 5% high GF showed the least suction compared to other flap heights. It can also be seen that the pressure gradients are mild for all the cases with the pressure continuously increasing till the trailing edge. It is also clear that the pressure recovery is not complete with the pressures on the upper and lower surfaces not becoming equal at the trailing edge, as is expected in this case, both with the GFs and without it. The pressure difference is the smallest for the cases without the GF, as expected.

On the lower surface, the pressures show a small increase with increasing GF height. Interestingly, for the smaller GF heights of 1% and 2%, the pressures closer to the leading edge are lower compared to the case without the GF. Away from the leading edge, the C_p values with the GF are higher compared to the case without the GF – a trend that was also reported by Maughmer and Bramesfeld [8].

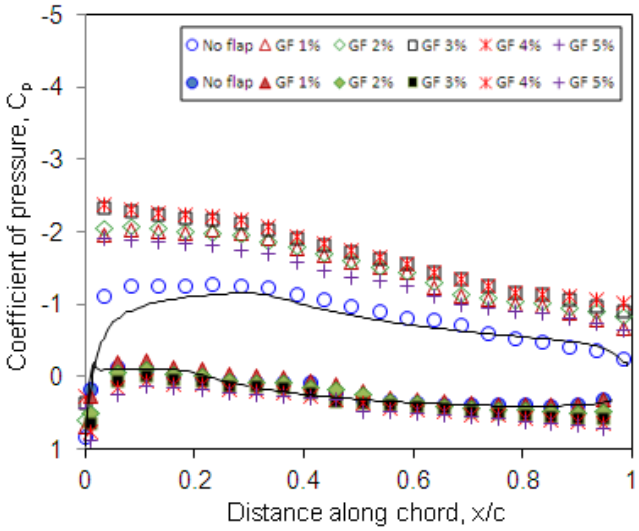

Fig. 3. Pressure distribution on the AF300 airfoil surface for $\alpha = 0^o$ and Re = 158,000 for different GF heights and without GF. The hollow symbols represent the suction side pressures and the solid symbols the pressure side. The continuous line shows the pressure distribution from CFX computations without GF

The streamlines around the airfoil for this case are shown in Fig. 4. As can be seen from the figures, the flow accelerates over the airfoil with the maximum velocity recorded at about 30% of chord. Close to the leading edge, the streamlines bunch together as a result of the reduction in the flow area and the velocity is seen to increase on both the sides. However, on the upper surface, the acceleration is much higher resulting in a considerable increase in velocity. On the lower surface, the flow starts to decelerate after some distance as the airfoil thickness reduces and the flow area increases. The development of the boundary layer can be seen on both the sides with the

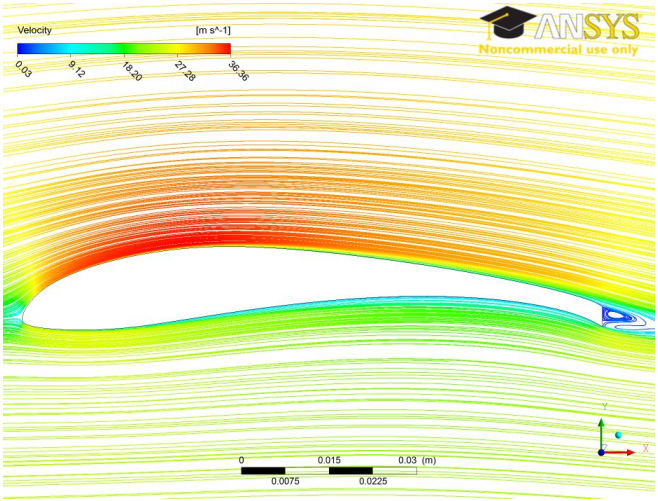

Fig. 4. The streamlines over the AF300 airfoil without GF for $\alpha = 0^o$ and Re = 158,000

lower surface boundary layer thicker at the trailing edge compared to the upper surface boundary layer. A vortex is seen to form right behind the blunt trailing edge.

The pressure distributions on the surface of the airfoil, obtained experimentally, for $\alpha = 4^o$ and Re = 158,000 for the cases without flap and with GFs of heights 1% to 5% are shown in Fig. 5. There is a significant increase in the suction on the upper surface for all the cases compared to the 0^o case, as is clear from a comparison with Fig. 3. Interestingly, the suction increases with the GF height till a height of 4% and then is the lowest for the 5% high GF. On the pressure side, the pressures increase slightly with all the GF heights close to the leading edge and by a larger amount towards the later portion of the chord. The pressures are highest for the 5% GF. The significant increase in the upper surface suction increases the C_l considerably (a finding reported by many researchers including ref. [1-8,25,26] and will be discussed later.

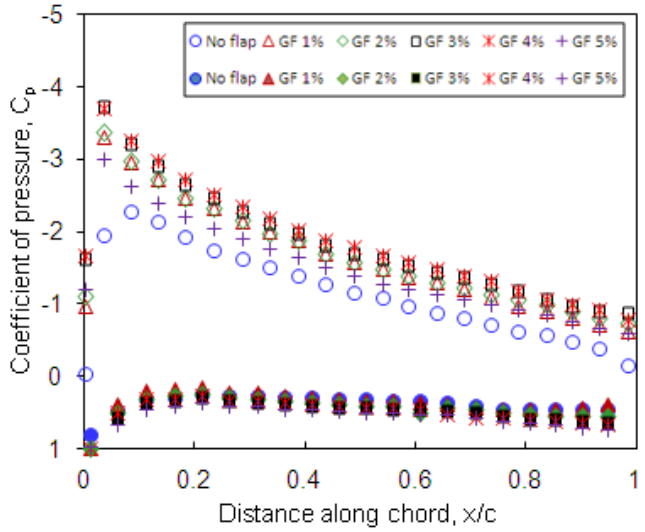

Fig. 5. Pressure distribution on the airfoil surface for $\alpha = 4^o$ and Re = 158,000 for different GF heights and without GF

When the angle of attack is increased to 8^o, which is the design angle of attack for this airfoil, there is a further increase in the suction on the upper surface both with and without the GFs, as shown in the experimental results in Fig. 6. Interestingly, again for the 5% high GF, the suction peak is lower compared to other GF heights. Moreover, for this GF height, the pressure recovery is faster initially and slows down towards the trailing edge. For this case, the total trailing edge thickness (including the GF) is 8% and the pressure recovery is expected to continue much downstream of the trailing edge. The CFX results for the 3% GF case are shown for comparison. A comparison with the CFX results for the 3% GF case is also made in this figure. It can again be seen that the suction peak as well as the suction for the first 20% of the chord from CFX is lower compared to the experimental one; beyond which there is a good match between the CFX and experimental pressure distributions on the upper surface – a trend that has been earlier [15] for almost all angles of attack till 18^o.

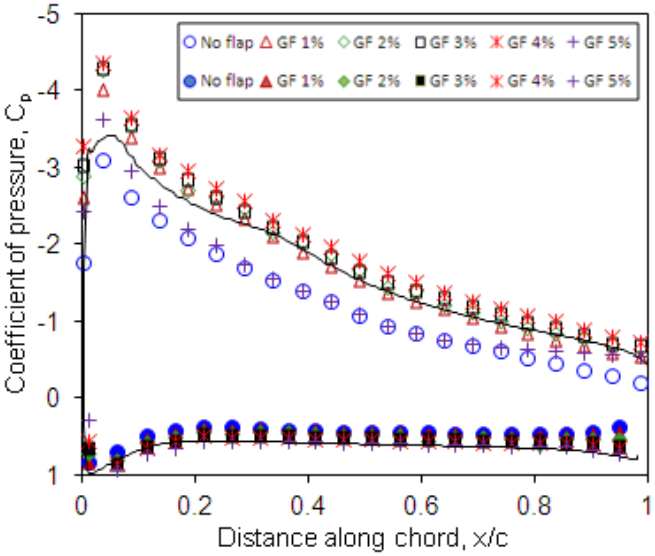

Fig. 6. Pressure distribution on the airfoil surface for $\alpha = 8^o$ and Re = 158,000 for different GF heights and without GF. The continuous line shows the pressure distribution from CFX computations for the 3% GF case

The iso-pressure contours were obtained for this angle of attack without GF and with the 3% GF. Figure 7 shows the iso-pressure contours for this angle without the flap. The pressure is high on the lower surface and reduces towards the trailing edge. The strong suction on the upper surface is also clear.

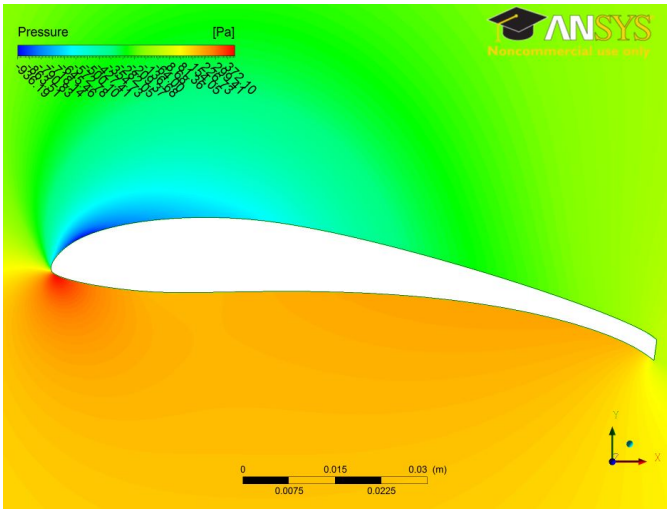

Fig. 7. Iso-pressure contours around the airfoil without GF for $\alpha = 8^o$ and Re = 158,000

The streamlines around the airfoil for $\alpha = 8^o$ and Re = 158,000 without flap are shown in Fig. 8. It can be seen that the peak velocity is reached very close to the leading edge.

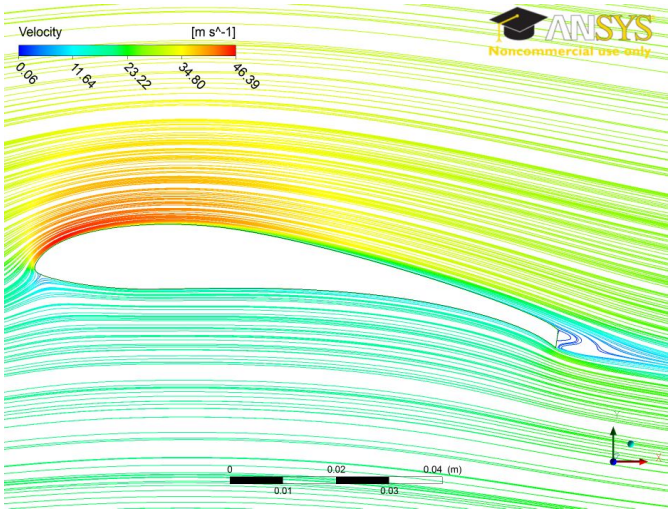

Fig. 8. The streamlines around the airfoil without GF for α = 8° and Re = 158,000

The iso-pressure contours for this angle and Re with the 3% GF are shown in Fig. 9. A significant increase in the pressure on the lower surface due to the retardation of the flow compared to the case without GF can clearly be seen from the figure. A comparison with Fig. 7 also shows that the suction peak has moved very close to the leading edge for the case with 3% GF height.

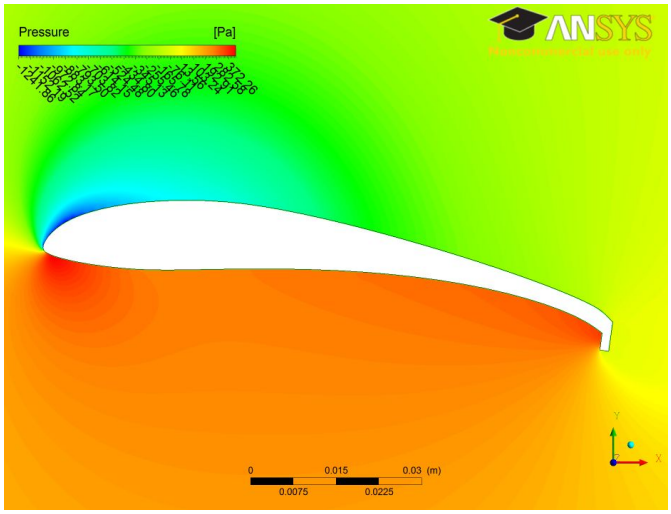

Fig. 9. Iso-pressure contours around the airfoil with 3% GF for α = 8° and Re = 158,000

The streamlines for this case are shown in Fig. 10. The retarded flow under the airfoil and the accelerated flow over the airfoil give rise to the significant pressure difference, resulting in a considerable increase in the lift force, compared to the case without flap. It should, however, be noted that CFX is not able to capture the suction peak accurately and under-predicted the C_l values compared to the experimental values.

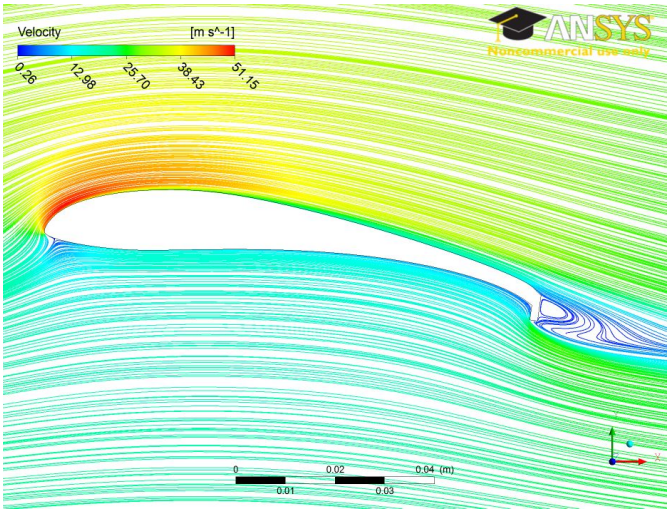

Fig. 10. The streamlines around the airfoil with 3% GF for α = 0° and Re = 158,000

The pressure distributions on the surface of the airfoil, obtained experimentally, for α = 12° and Re = 158,000 for all the GF heights and without the GF are shown in Fig. 11. Interestingly, for this case, the upper surface suction is not significantly higher compared to the 8° case both with and without the flap. However, the pressure on the lower surface is higher for all the cases, as can be seen from the figure.

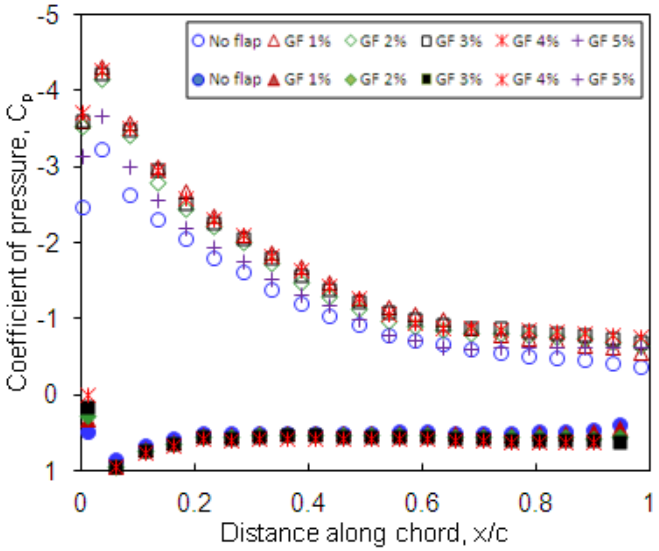

Fig. 11. Pressure distribution on the airfoil surface for α = 12° and Re = 158,000 for different GF heights and without GF

The transition of the upper surface boundary layer occurs at about 0.4c for the angle of attack of 4° and moves upstream to about 0.16c for α = 8° and Re = 158,000. The location of transition moves further upstream to 0.1c at α = 12°. Figure 12 shows the turbulent kinetic energy distribution over the airfoil for α = 8° and Re = 158,000 without the GF. The location of transition can be seen from this figure.

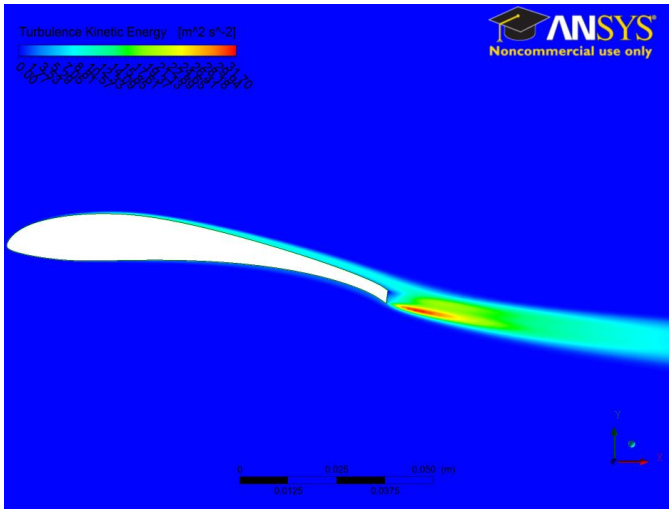

Fig. 12. The turbulent kinetic energy around the airfoil without GF for $\alpha = 8^o$ and Re = 158,000

The location of transition is a very important factor that significantly influences the performance of the airfoil. The distance from the leading edge to the point where transition occurs, x_{tr}, reduces with a) increasing Re, and b) increasing turbulence intensity. Also, when the blade leading edge gathers dust, dirt etc., it causes early transition of the boundary layer. As x_{tr} reduces, the region of laminar boundary layer reduces and that of turbulent boundary layer increases; this results in an increase in the skin friction drag. For higher α, the shift in the location of transition is normally less as the transition anyway occurs close to the leading edge. However, for higher α, a reduction in x_{tr} may shift the location of separation towards the trailing edge, resulting in a reduction in the wake thickness and a lower momentum loss [22,27]. Interestingly, for $\alpha = 8^o$ and Re = 158,000, the transition point for the airfoil with 3% GF moved right at the leading edge.

The variations of the experimental coefficient of lift, C_l, with angle of attack for different GF heights are shown in Fig. 13. The lift coefficient increases with angle of attack till 12^o. This airfoil was found to stall at 14^o; hence the C_l values at 16^o drop. The effect of GF was not studied for the angle of attack of 14^o. It is interesting to note from the pressure distributions reported earlier that the increase in C_l for the cases with GFs has contributions from both the upper and lower surfaces. Compared to the case without GF, the C_l value of the airfoil with 1% GF increases significantly due to the considerably higher suction on the upper surface – especially near the leading edge. For other GF heights, the increase compared to 1% GF is not much because the suction does not increase much; however, there is contribution from the lower surface which increases with increasing height of the GF. Similar results were reported by Li et al. [26] for angles of attack of 0^o, 6^o and 10^o, who recorded an increase in suction on the upper surface and an increase in pressure on the lower surface for NACA0012 airfoil with a 2% GF.

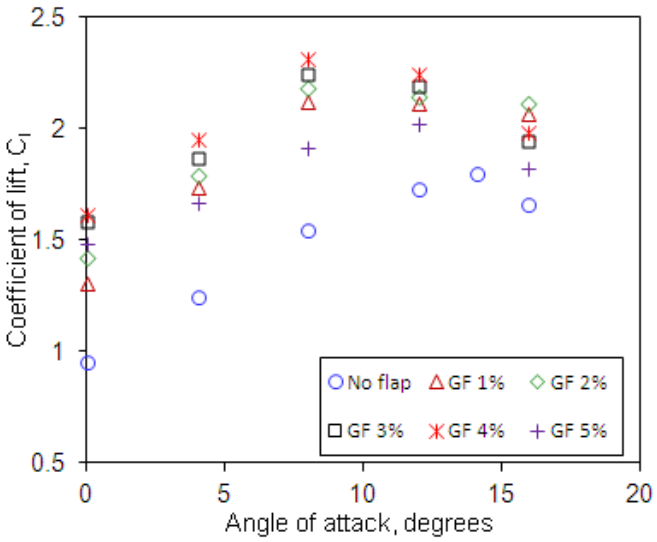

Fig. 13. Coefficient of lift at different angles of attack at Re = 158,000 for different GF heights and without GF

For the angle of attack of 10^o, there was a significant increase in the suction peak similar to the increase reported here.

The variations of the coefficient of drag, C_d, with angle of attack for different GF heights are shown in Fig. 14. Interestingly, the coefficient of drag does not change much with GF height as well without GF for $\alpha = 0^o$. This is mainly due to the geometry of the airfoil; at $\alpha = 0^o$, the increase in the suction on the upper surface close to the leading edge reduces the drag because the force in that area has a strong component in the negative drag direction. Similarly, on the lower surface between 0.2c and 0.5c, the pressure force has a component in the negative drag direction. These components cancel out the contribution to the positive drag from the rear half of the airfoil.

As the angle of attack is increased, this "advantage" of negative drag contribution from the front half of the airfoil reduces and the drag starts to increase both due to the higher suction from the rear portion of the airfoil as well as due to the higher pressure on the entire lower surface which have components in the positive drag direction. Thus, it can be seen that at $\alpha = 8^o$ and beyond, the drag penalty due to the increased GF height increases considerably compared to 0^o and 4^o. The drag increases significantly at $\alpha = 16^o$ because of the flow separation from the upper surface.

The maximum lift-to-drag ratio for $\alpha = 8^o$ was recorded for the GFs of 1% and 2%. Interestingly, the lift-to-drag ratio does not change significantly when the angle of attack is reduced to 4^o or increased to 12^o for these two GF heights, which makes it an attractive option to operate this blade at 8^o. Any sudden change in the flow direction within that range of angles of attack or the flow velocity will still give similar lift-to-drag ratio, which will ensure a consistently good output from the wind turbine.

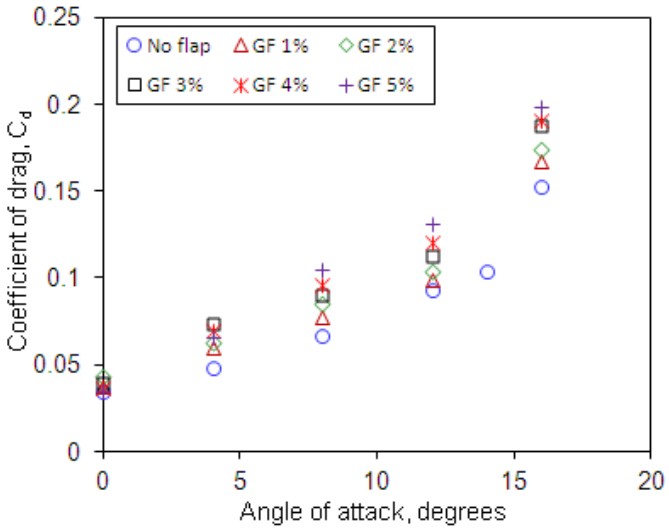

Fig. 14. Coefficient of drag at different angles of attack at Re = 158,000 for different GF heights and without GF

However, when the angle of attack is further increased from 16° to 20°, the C_l value drops from about 1.66 to to about 1.48, while the C_d value rises from 0.153 to 0.18 for Re = 158,000.

EFFECT OF REYNOLDS NUMBER

The experiments were performed at three Reynolds numbers, as mentioned earlier. It was interesting to find that in most of the cases without GF, no major difference in the pressure distributions or the lift and drag behavior was recorded, except for a small increase in the C_l values when Re was increased from 128,000 to 205,000 for a given angle of attack [15]. Even for the angle of attack of 14°, the pressure distributions on the airfoil surface for the two Re almost coincide with a negligible difference in the C_l and C_d values. Similar trends were observed in the present case even with the GF of different heights. Figure 15 shows the pressure distributions on the surface of the airfoil α = 0° and Re = 250,000. A comparison with Fig. 3 shows that there is a small increase in the suction on the upper surface (except for the 5% GF which showed strong suction) and a small reduction in the pressure on the lower surface. Thus, the C_l values remain nearly the same for both the Reynolds numbers. There was no significant difference in the drag coefficient as well when Re was changed from 100,000 to 250,000. Similar results were reported for this airfoil without GF for Re values of 128,000 and 205,000 with C_d remaining essentially constant with increasing Re [15].

The effect of Re on this airfoil was further investigated by increasing Re to 800,000 for the case of α = 8° and a GF height of 3%. It was interesting to find from the CFX results for this case that the pressure distribution still does not show any significant difference compared to lower Re; the C_l and C_d values varied by less than 1% compared to Re = 250,000.

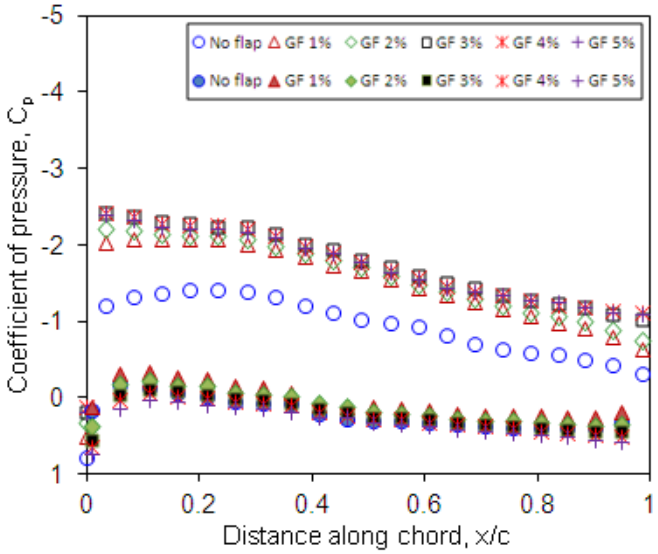

Fig. 15. Pressure distribution on the AF300 airfoil surface for α = 0° and Re = 250,000 for different GF heights and without GF.

EFFECT OF TURBULENCE INTENSITY

The freestream turbulence intensity was increased from 1% to 10% to study its effect on the aerodynamic characteristics. The effect of turbulence level for α = 8° and Re = 158,000 without the GF is shown in Fig. 16. It can be seen that the suction on the upper surface is slightly stronger at the higher turbulence level – a phenomenon commonly observed and reported in the past [18,22,27]. Also, the pressure on the lower surface is higher at the higher turbulence level. As a result, the C_l value for the higher turbulence level is higher compared to the lower turbulence level of 1%. However, the drag coefficient also increases slightly for the higher turbulence level. For this particular case, C_d increased by nearly 14% at Tu = 10%.

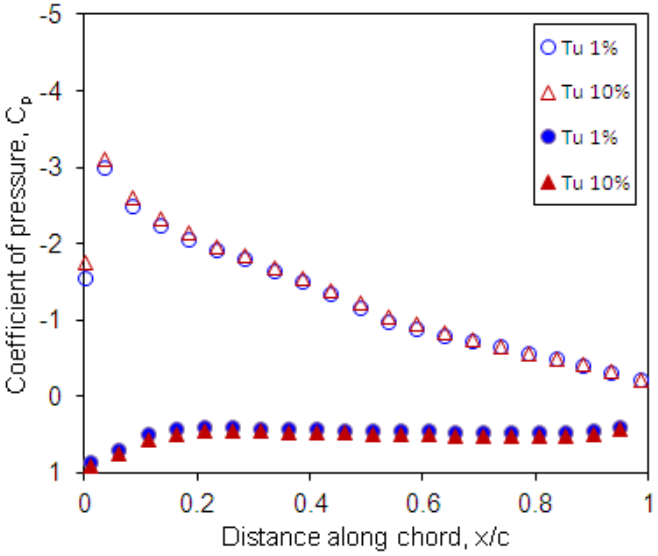

Fig. 16. Effect of turbulence intensity on the pressure distribution on the airfoil without GF for α = 8° and Re = 158,000.

The most interesting observation for the case with higher Tu was the location of transition which moved right to the leading edge as shown in Fig. 17; an observation that was also made for this angle at 1% turbulence intensity with the 3% high GF. Devinant et al. [18] reported shifting of the location of transition right up to the leading edge at high turbulence levels of the freestream flow. A turbulent boundary layer is known to be thicker and causes a higher skin friction drag [18]. The thicker boundary layer for the case of 10% freestream turbulence intensity (Fig. 17) compared to the turbulence intensity of 1% (Fig. 12) resulted in the higher drag coefficient mentioned above.

For the case with GF, the pressure distributions at $\alpha = 8^o$ and Re = 158,000 for the 3% GF for the two turbulence levels are shown in Fig. 18.

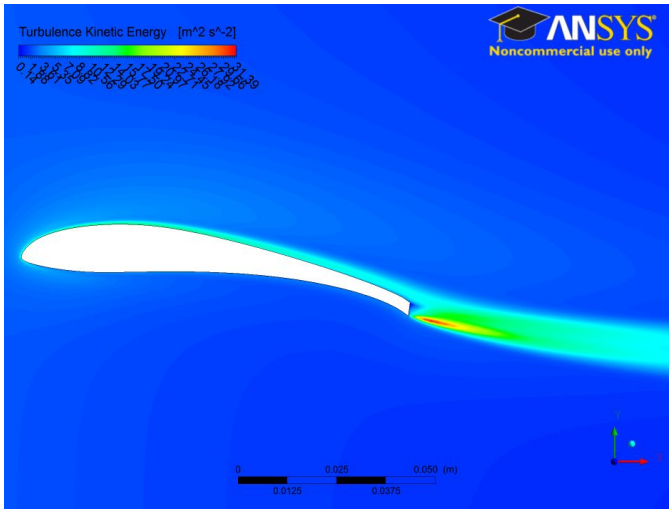

Fig. 17. The turbulent kinetic energy around the airfoil without GF for $\alpha = 8^o$ and Re = 158,000 and Tu = 10%.

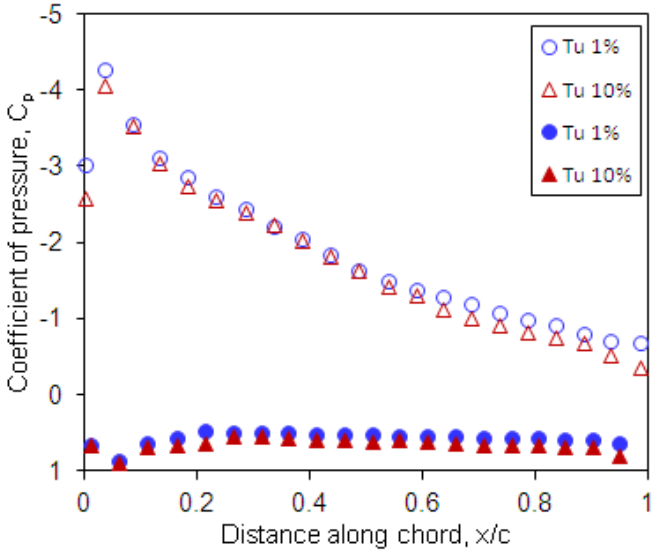

Fig. 18. Effect of turbulence intensity on the pressure distribution on the airfoil with 3% GF for $\alpha = 8^o$ and Re = 158,000.

It can be seen that the higher turbulence has resulted in a small reduction in the suction on the upper surface, while there is an increase in the pressure on the lower surface. As a result, there is a small increase in the lift coefficient. A reduction in the suction is not normally observed for sharp trailing-edge airfoils with an increase in the freestream turbulence level, e.g. ref. [27], where an increase in suction on the upper surface with an increase in the freestream turbulence for all the cases studied was reported. However, Swalwell et al. [17] did observe a small reduction in the upper surface suction at a Tu of 7% compared to a Tu of 4% for NACA0021 airfoil.

CONCLUSIONS

Detailed investigation of the effect of adding a Gurney flap to a thick trailing-edged airfoil was performed experimentally and numerically. It was found that

(a) the Gurney flap significantly improves the suction on the upper surface of the airfoil.

(b) there is an increased pressure on the lower surface with the Gurney flap in the second half of the airfoil chord.

(c) for most of the angles of attack and Reynolds numbers, the suction on the upper surface increased as the Gurney flap height was increased from 1% to 4% of chord. However, for the 5% flap, the suction was found to be lower compared to the lower flap heights.

(d) the coefficient of lift increased linearly up to an angle of attack of 14% without the Gurney flap. With the Gurney flap, the maximum lift coefficient was recorded at 8^o.

(e) the Reynolds number does not have a strong influence on the flow and the lift and drag characteristics in the range of Re = 100,000 to 250,000. Even an increase in Re up to 800,000 did not result in any significant change in the lift and drag coefficients.

(f) the maximum lift-to-drag ratio for $\alpha = 8^o$ was recorded for the GFs of 1% and 2%. Interestingly, the lift-to-drag ratio does not change significantly when the angle of attack is reduced to 4^o or increased to 12^o for these two GF heights, which makes it an attractive option to operate this blade at 8^o.

ACKNOWLEDGEMENT

The authors wish to thank the technical staff Mr. Sanjay Singh and Mr. Shiu Prasad during the construction of the models and setting up of the experiments. The authors are also thankful to Mr. Victor Hoasirao and Mr. Kaushik Sharma for their help during the experimental work and to Mr. Deepak Prasad during the computational work.

REFERENCES

[1] Liebeck, R.H., 1978, "Design of subsonic airfoils for high lift", *Journal of Aircraft*, **15**, 547-561.

[2] Wang J.J., Li, Y.C., and Choi, K.-S., 2008, "Gurney flap – Lift enhancement, mechanisms and applications", *Progress in Aerospace Sciences*, **44**, 22-47.

[3] Kentfield, J.A.C., Clavelle, E.J., 1993, "The flow physics of the Gurney flaps devices improving turbine blade performance", *Wind Engineering*, **17**, 24-34.

[4] Kentfield, J.A.C., 1994, "Theoretically and experimentally obtained performances of Gurney-flap equipped wind turbines", *Wind Engineering*, **18**, 63-74.
[5] Bao, N., Ma, H. and Ye, Z., 2000, "Experimental study of wind turbine blade power augmentation using airfoil flaps", *Wind Engineering*, **24**, 25-34.
[6] Berg, D., Johnson, S.J, Van Dam, C.P., 2008, "Active load control techniques for wind turbines", *Sandia Report SAND2008-4809*.
[7] Altmann, G.F., 2011, "An investigative study of Gurney flaps on a NACA0036 Airfoil", MSc Dissertation, California Polytechnic State University, CA.
[8] Maughmer, M.D. and Bramesfeld, G., 2008, "Experimental investigation of Gurney flaps", *Journal of Aircraft*, **45**, 2062-2067.
[9] Day, A.H. and Cooper, C., 2011, "An experimental study of receptors for drag reduction on high-performance sailing yachts", *Ocean Engineering*, **38**, 983-994.
[10] Abbott, I.H. and Van Doenhaff, A.E., 1958, *Theory of Wing Sections,* Dover Publications Inc., New York, p. 100, pp. 452-687.
[11] Fupeng, H., Yuhong, L. and Zuoyi, C., 2001, "Suggestions for improving wind turbines blade characteristics", *Wind Engineering*, **25**, 105-113.
[12] Xuan, H., Weimin, Z., Xiao, L. and Jieping, L., 2008, "Aerodynamic and aeroacoustic optimization of wind turbine blade by a genetic algorithm", *Proceedings of 46th AIAA Aerospace Sciences Meeting and Exhibit*, Reno, Nevada, AIAA-2008-1331.
[13] Selig, M.S. and McGranahan, B.D., 2004, "Wind tunnel aerodynamic tests of six airfoils for use on small wind turbines", *NREL Report SR-500-34515*.
[14] Giguerre, P. and Selig, M.S., 1997, "Low Reynolds number airfoils for small horizontal axis wind turbines", *Wind Engineering*, **21**, 367-380.
[15] Singh, R.K., Ahmed, M.R. and Lee, Y.-H., 2012, "Design of a low Reynolds number airfoil for small horizontal axis wind turbines", *Renewable Energy*, **42**, 66-76.
[16] Hoffmann, J. A., 1991, "Effect of freestream turbulence on the performance characteristics of an airfoil", *AIAA Journal*, **29**, 1353-1356.
[17] Swalwell, K. E., Sheridan, J. and Melbourne, W. H., 2001, "The effect of turbulence intensity on stall of the NACA 0021 aerofoil", *Proc. 14th Australasia Fluid Mechanics Conference*, Adelaide, 941-944.
[18] Devinant, Ph. Laverne, T., Hureau, J., 2002, "Experimental study of wind-turbine airfoil aerodynamics in high turbulence," *Journal of Wind Engineering and Industrial Aerodynamics*, **90**, 689-707.
[19] Maeda, T., Kamada, Y., Murata, J., Toki, T. and Tobuchi, A., 2010, "Effect of turbulence intensity on dynamic characteristics of wind turbine airfoil", *Proc. of RE2010 Conference*, Yokohama, Japan, Paper No. P-Wd-36.
[20] Sicot, S., Devinant, P., Laverne, T., Loyer, S. and Hureau, J., 2006, "Experimental study of the effect of turbulence on horizontal axis wind turbines", *Wind Energy*, **9**, 361-370.
[21] Garratt, J.R. and Taylor, P.A., 1996, *Boundary-Layer Metereology*, Kluwer Academic Publishers, Netherlands, 300-318.
[22] Ahmed, M. R., 2012, "Blade sections for wind turbine and tidal current turbine applications – current status and future challenges", *International Journal of Energy Research*, **36**, 829-844.
[23] Baker, J.P., Mayda, E.A. and van Dam, C.P., 2006, "Experimental analysis of thick blunt trailing-edge wind turbine airfoils", *ASME Journal of Solar Energy Engineering*, **128**, 422-431.
[24] Barlow, J. B., Rae, W. H. Jr., Pope, A., 1999, *Low Speed Wind Tunnel Testing*, Wiley Interscience, New York, 349-363.
[25] Storms, B.L. and Jang, C.S., 1994, "Lift enhancement of an airfoil using a Gurney flap and vortex generators", *Journal of Aircraft*, **31**, 542-547.
[26] Li, Y. C., Wang, J.J. and Zhang, P.F., 2002, "Effect of Gurney flaps on a NACA0012 airfoil", *Flow, Turbulence and Combustion*, **68**, 27-39.
[27] Ahmed, M. R., Narayan, S., Zullah, M. A. and Lee, Y. –H., 2011, "Experimental and numerical studies on a low Reynolds number airfoil for wind turbine blades", *Journal of Fluid Science and Technology*, **6**, 357-371.

